Since January 2020 Elsevier has created a COVID-19 resource centre with free information in English and Mandarin on the novel coronavirus COVID-19. The COVID-19 resource centre is hosted on Elsevier Connect, the company's public news and information website.

Sustainable Cities and Society 75 (2021) 103408

Contents lists available at ScienceDirect

Sustainable Cities and Society

journal homepage: www.elsevier.com/locate/scs

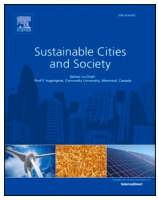

Effective ventilation and air disinfection system for reducing coronavirus disease 2019 (COVID-19) infection risk in office buildings

Shubham Srivastava [a,1], Xingwang Zhao [b,1,*], Ati Manay [a], Qingyan Chen [c]

[a] Water Heater Division, Rheem Manufacturing Company Inc, Atlanta, GA 30328, USA
[b] School of Energy and Environment, Southeast University, Nanjing 210096, China
[c] School of Mechanical Engineering, Purdue University, West Lafayette, IN 47907, USA

ARTICLE INFO

Keywords:
Airborne transmission
COVID-19
Infection risk
Indoor environment
CFD
Ultraviolet-C disinfection device

ABSTRACT

During the COVID-19 pandemic, an increasing amount of evidence has suggested that the virus can be transmitted through the air inside buildings. The ventilation system used to create the indoor environment would facilitate the transmission of the airborne infectious diseases. However, the existing ventilation systems in most buildings cannot supply sufficient clean outdoor air for diluting the virus concentration. To reduce the airborne infection risk and minimize energy consumption, especially in existing buildings with well-mixed ventilation systems, this investigation used an ultraviolet-C (UV-C) air disinfection device (Rheem's third generation products, RM3) with 99.9% disinfection efficiency to clean air carrying the COVID-19 virus (severe acute respiratory syndrome coronavirus 2, SARS-CoV-2) which could help promote environmental sustainability and create healthy cities. This investigation assessed the impact of the RM3 UV-C units on the infection risk, the number of RM3 UV-C units required, and the strategy for decreasing the infection risk, with the use of computational-fluid-dynamics (CFD) numerical simulations. An actual office building with a combination of individual offices and workstations was selected as an example for the research. According to the numerical results, the best strategy would be to use a combination of 100% outside air and UV-C in heating, ventilation and air-conditioning (HVAC) ducts with air disinfected by the RM3 UV-C units. The infection risk in the office building could thus be reduced to a negligible level. These findings could provide theoretical basis and engineering application basis for COVID-19 epidemic prevention and control.

1. Introduction

Since the outbreak of COVID-19 in 2019, more and more evidence has suggested that the virus can be transmitted through the air from a sick patient and that the virus in small aerosol droplets can survive in the air for hours (Doremalen et al., 2020; Liu et al., 2020; Morawska & Cao, 2020). Some studies have also indicated that the ventilation systems (Ding et al., 2020; Pei et al., 2021) used to create the indoor environment in buildings would affect the transmission of airborne infectious diseases (Blocken et al., 2021; Li et al., 2007). For example, in a Dutch nursing home, 17 out of 21 residents and 13 out of 34 healthcare workers wearing surgical masks in the same ward were infected. In addition, to save energy, this ward was ventilated using recirculated air without filtration when the CO_2 concentration was lower than 1000 ppm. However, the occupants of six other wards ventilated by outside air in the same facility were not infected. The researchers' findings indicated that the airborne transmission (Crema, 2021; Rahmani et al., 2020; Yao et al., 2020) resulted from an inadequate supply of outside air (Man et al., 2020). The outside air supply rate to offices, conference rooms, shops, libraries, restaurants, etc., was much lower than that in hospitals, and thus the infection probability in those spaces would be higher. The epidemiologic analysis, experimental measurements, and simulation results from Li et al. (2021) indicate the high probability of airborne transmission in a poorly ventilated and crowded restaurant. Moreover, people spend more than 87% of their daily lives inside buildings (Klepeis et al., 2001). It is particularly important to improve air quality indoors (Agarwal et al., 2021; Cao et al., 2020) and reduce indoor exposure to airborne infectious diseases (Kenyon et al., 1996; Moser et al., 1979; Olsen et al., 2003) in the existing buildings.

To improve indoor air quality during the COVID-19 pandemic, the

* Corresponding author.
E-mail address: xw_zhao@seu.edu.cn (X. Zhao).
[1] These authors contributed equally to this work and should be considered co-first authors.

https://doi.org/10.1016/j.scs.2021.103408
Received 18 July 2021; Received in revised form 24 September 2021; Accepted 25 September 2021
Available online 29 September 2021

most common recommendation has been to supply sufficient outdoor air to minimize the infection risk of COVID-19 in buildings (ASHRAE, 2020; CDC, 2020; European Centre for Disease Prevention & Control, 2020). More fresh air needs extra energy to handle outdoor air, such as heating, cooling and (de)humidifying. However, not all the ventilation systems in buildings can handle the heating and cooling load with 100% outside air. There are no ventilation standards for the amount of outdoor air required in buildings for the control of SARS-CoV-2 infection (American Society of Heating, 2019). Other studies (Feng et al., 2021a; Rahmani & Mirmahaleh, 2021; Xu, Luo, Yu, & Cao, 2020) have proposed intermittent occupancy with ventilation (Melikov et al., 2020), a decrease in occupancy density (Wang et al., 2021), or a reduction of working hours (Zhang et al., 2020). All these measures could help in principle, but they are not permanent solutions. The purpose of the present investigation was to provide a simple and energy saving method for reducing the SARS-CoV-2 infection risk with minimal changes to existing ventilation systems, so as to create a healthy indoor environment and enable people to return to work.

One promising technique is the use of local air cleaning systems (Morawska & Milton, 2020) in combination with ventilation. Therefore, this investigation aims to using an ultraviolet-C (UV-C) disinfection device to clean air carrying SARS-CoV-2. To assess the virus airborne transmission mechanism and the performance of the device, this study calculated the infection risk with the spatial distribution of SARS-CoV-2 in a large office building.

2. Methods

To investigate the infection risk of SARS-CoV-2 in a large office building and the performance of the disinfection device, this study would firstly validate the numerical simulation method with experimental data. Then the validated simulation method was used to solve N-S equation for the flow field and Eulerian method was used to predict the spatial distribution of the SARS-CoV-2 virus concentration. With the SARS-CoV-2 virus concentration, this investigation further adopted the Wells-Riley equation to evaluate the spatial distribution of the infection risk and explore the effect of air disinfection device on reducing the probability of infection.

2.1. Airflow and turbulence model

The investigation used computational fluid dynamics (CFD) to calculate the spatial distributions of airflow (Chen et al., 2021; Ren & Cao, 2021), air temperature, and SARS-CoV-2 concentration (Ren & Cao, 2020; Ren et al., 2021) in an office building. Accurate prediction of indoor airflow distribution is essential for studying the spatial distribution and transmission of airborne infectious diseases. The indoor air distribution in this study was predicted by CFD solving the Reynolds-averaged Navier-Stokes (RANS) equations closed with the renormalization group (RNG) k-ε model (Choudhury, 1993). This turbulence model has the best perforpance among many evaluated in the literature (Chen, 1995; Zhang et al., 2007) for airflow in the indoor environment.

To predict the spatial distribution of SARS-CoV-2 in a large office building, both Euler's method (Guo et al., 2021; Liu, Li, Wu, Ju, & Gao, 2021; You, Lin, Wei, & Chen, 2019; Zhang & Chen, 2007) and Lagrangian method with CFD are widely used. However, Lagrangian method may not be easy to achieve a stable solution for different factors, such as the number of the released virus, uncertainty, and random factors (Zhang & Chen, 2007). So, this investigation used the Eulerian method for the further study.

2.2. Eulerian method

The Eulerian method treats the particle (droplet or virus) phase as a continuum phase and solves the spatial distribution of SARS-CoV-2 virus by solving the following scalar transport equation:

$$\frac{\partial \rho \Phi}{\partial t} + \frac{\partial}{\partial x_i}(\rho \Phi U_i) = \frac{\partial}{\partial x_j}\left(\Gamma_\Phi \frac{\partial \Phi}{\partial x_j}\right) + S_\Phi \quad (1)$$

where Φ is the SARS-CoV-2 quanta concentration, t is time, x_i and x_j are coordinates in the i and j directions, respectively, ρ is air density, U_i is air velocity, Γ_Φ is the diffusion coefficient, and S_Φ is the quantum generated by an index patient. Here "quanta" are the hypothetical infectious dose units proposed by Wells (1955) and used to signify the strength of the infection produced by an infected patient. The quanta are usually back-determined from the outbreak cases. This investigation used ANSYS (2010), a widely used commercial CFD program, to predict indoor air distributions (Cao, 2018; Feng et al., 2019) and quanta concentration. Since it is commercial software, the source code cannot be modified directly. User defined function (UDF) always needs to be written by users according to requirements and connected with the software through the interface provided by the software. For solving Eq. (1), this study ignored the Brownian diffusivity and adopted the homogeneous assumption which assume the Stokes number of a particle equal zero. The turbulent Schmidt number was set at 1.0 (You et al., 2019). All the above assumptions were used in previous studies (Guo, Qian, Sun, Cao, & Zhang, 2021; Liu, Li, Wu, Ju, & Gao, 2021; You et al., 2019; Zhang & Chen, 2007). This study first employed the finite volume method to discretize the RANS equations closed with the RNG k-ε model and Eq. (1), and then solved the discretized equations with the SIMPLE algorithm (Patankar & Spalding, 1972). To simulate the buoyancy effect, Boussinesq approximation (Boussinesq, 1903) was adopted in this investigation. All the CFD simulations were conducted on a computer cluster with 128 processor cores (processor base frequency: 2.0 GHz) and 256 GB of memory.

2.3. Wells-Riley equation

To assess the quantitative infection risk, the spatial distribution of SARS-CoV-2 quanta calculated by CFD was used in the Wells-Riley equation and the dose-response model (To & Chao, 2009). The Wells-Riley equation was first proposed by Riley et al. (1978) to assess the infection risk during the measles pandemic in 1978. (Liu, Li, Wu, Ju, & Gao, 2021) used a modified Wells-Riley equation to study the impacts of different dividers on the infection risk in restaurant environments. However, their results shows that this method will make the virus stay in the partition space and infect the next person. Guo et al. (2021) only developed a new rapid method to access the spatial distribution of infection risk based on the fixed air flow pattern when the occupants' locations are variable. This investigation tried to propose an energy saving equipment to deal with the SARS-CoV-2 virus and predict the infection risk by employing the Wells-Riley equation. Dai and Zhao (2020) estimated the quanta value for COVID-19 that was used for this study.

Under the assumption of a fully mixed state, the Wells-Riley equation estimates the average infection risk probability P and average quanta concentration Φ_{avg} in the office building as a whole through Eqs. (2) and (3). Both P and Φ_{avg} are affected mainly by the clean air ventilation rate Q.

$$P = 1 - e^{-Iqpt_1/Q} \quad (2)$$

$$\Phi_{avg} = Iq/Q \quad (3)$$

where I represents the number of index patients; q the quanta produced by each patient (h^{-1}); p the pulmonary ventilation rate of each susceptible person (m^3/h), in a seated position or doing light activity, $p = 0.3$ m^3/h; t_1 the duration of exposure (h); and Q the ventilation rate of clean air supplied to the room (m^3/h). The quanta range for COVID-19 estimated by Dai and Zhao (2020) was 14–48 h^{-1}, and this investigation used the median value of 31 h^{-1}. This study assumed that each

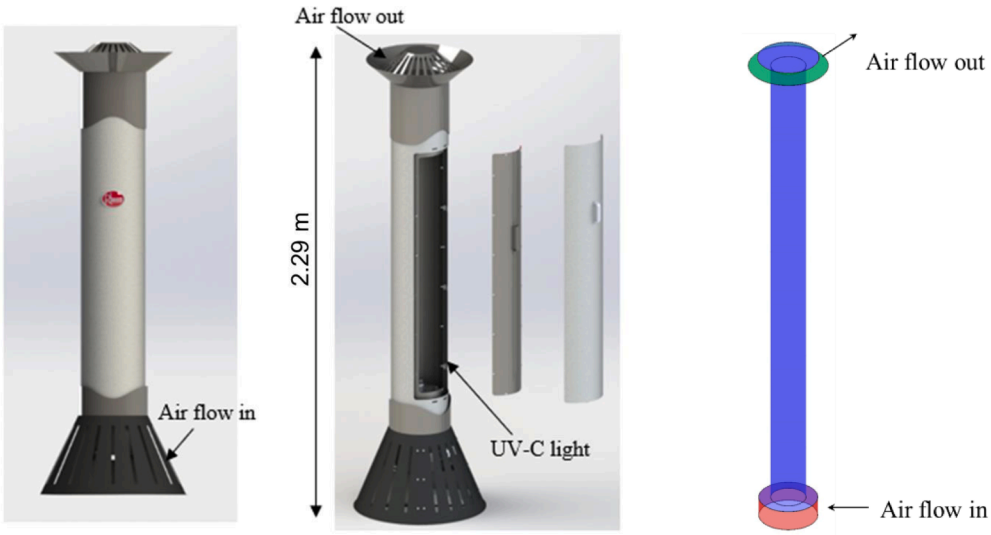

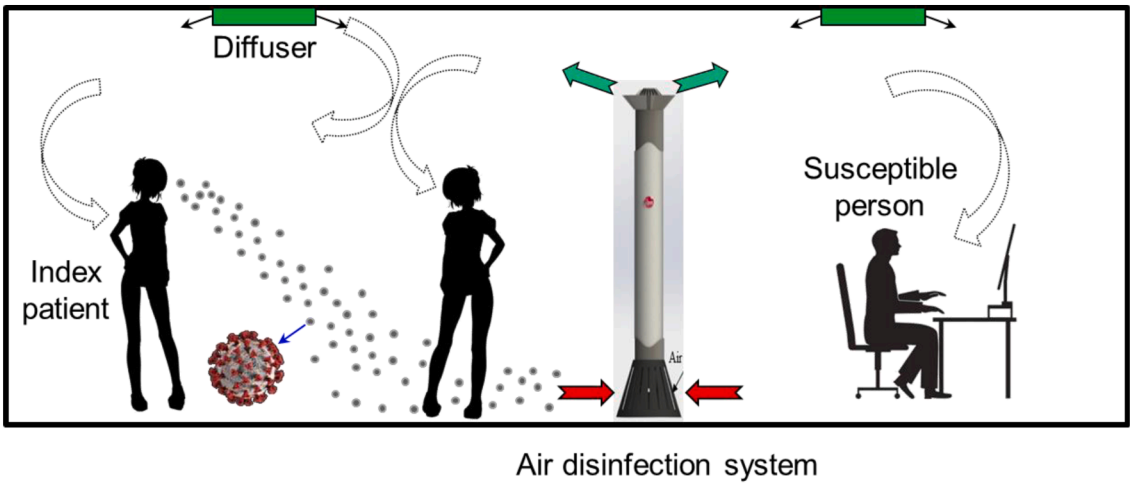

Fig. 1. (a) Physical model of RM3 UV-C air disinfection unit, (b) simplified model of the RM3 unit used for CFD simulation, and (c) an RM3 UV-C unit installed in an office with mixing ventilation.

susceptible person was exposed for 8 h in an office and that the office space had four infected occupants.

To solve the individual infection risk probability for each person, this study needed to determine the local average quanta concentration $\Phi_{k,\theta}$ in the breathing zone θ of person *k*. Based on the CFD simulation results, this investigation calculated the local average quanta concentration $\Phi_{k,\theta}$ by means of Eq. (4). The breathing zone θ was assumed to be a spherical space centered at the nose of each person, with a radius of 0.2 m which was determined according to Shi et al.'s (2019) study.

$$\Phi_{k,\theta} = \frac{\sum_{ii=1}^{ii=m} \Phi_{k,ii} \cdot Vol_{k,ii}}{\sum_{ii=1}^{ii=m} Vol_{k,ii}} \tag{4}$$

where $\Phi_{k,ii}$ and $Vol_{k,ii}$ are the quanta concentration and volume of cell *ii* in the breathing zone θ, respectively; and *m* is the total number of cells in the breathing zone. With the average quanta concentration in each susceptible person's breathing zone, this investigation then estimated the infection risk for each susceptible person P_k through the following equation:

$$P_k = 1 - e^{-\Phi_{k,\theta} p t_1} \tag{5}$$

2.4. RM3 UV-C unit for localized air disinfection

An effective method for reducing the infection risk for each susceptible person is to increase the number of air changes per hour (ACH) in an indoor space. However, this approach causes a steep rise in HVAC operating costs. The same objective can be achieved by installing localized air disinfection devices.

The localized air-cleaning techniques include air purifiers with fibrous filter, electrostatic removal system (Mo et al., 2020), UV system, etc. HEPA filters are commonly used for particles filtration (Ding et al., 2020). However, the first two methods have re-aerosolization and electric breakdown risks. Heilingloh et al. (2020) studied the sensitivity of SARS-CoV-2 to ultraviolet light, their results shows that ultraviolet light can quickly inactivate SARS-CoV-2. Casini, Tuvo, & Cristina, 2019

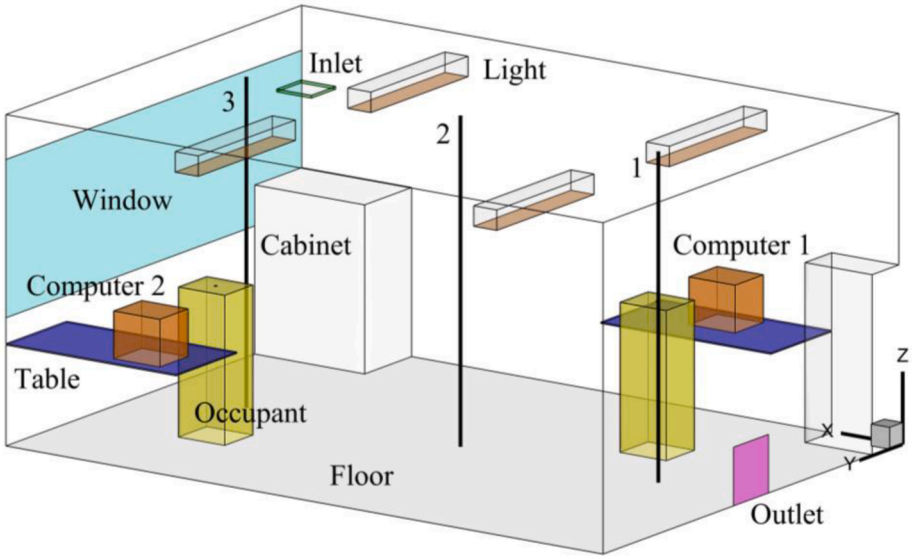

(a) Schematic view of the environmental chamber

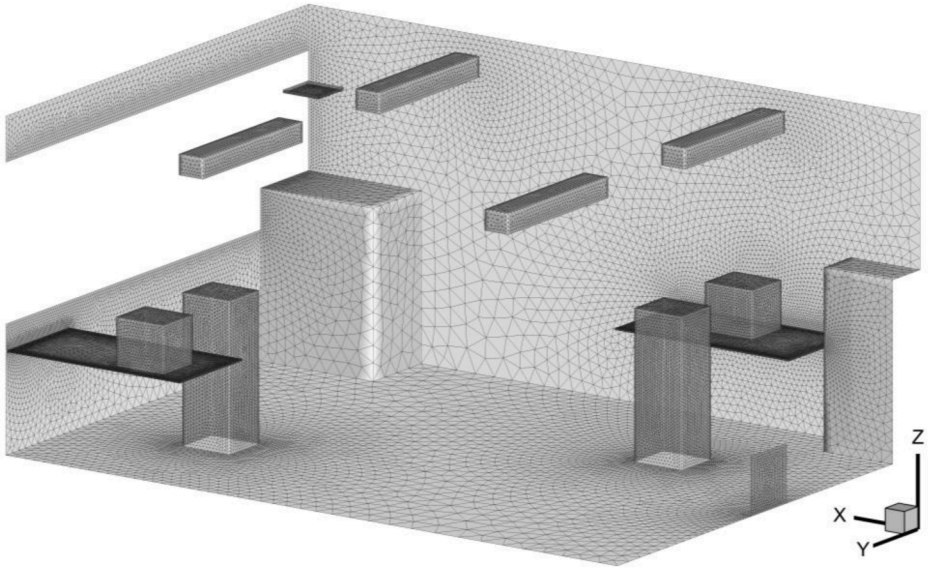

(b) Boundary mesh information

Fig. 2. Schematic view of the environmental chamber from Srebric and Chen (2002) and mesh information.

study shows that UV-C can effectively reduce the probability of infection on high-touch surfaces. (Feng et al., 2021b) also indicated that UV is the most reliable and safe method which is suitable for different indoor environment, such as hospital, office building, school, et al. All these studies (Feng et al., 2021b; Heilingloh et al., 2020; Nakpan et al., 2019) indicated that UV-C can be used to against SARS-CoV-2, so this investigation developed an RM3 UV-C units with ultraviolet germicidal irradiation (UVGI) technology to sanitize the recirculating air for reducing the infection risk during the epidemic period.

The UVGI light in this investigation employed the short-wavelength UV-C range, from 100 to 280 nm, as the principal mode for disinfecting from the SARS-CoV-2 virus. It works by permanently destroying the DNA structure of the pathogens, rendering them non-virulent. Fortunately, the SARS-CoV-2 has been found to be particularly susceptible to radiation in this range (Narita et al., 2020). Note that, UV-C light, although being fatal to microorganisms, does not pose significant health risks to humans (Buonanno et al., 2017). The aim of using the RM3 UV-C unit was to kill 99.9% of the viruses (kill efficiency $\eta = 99.9\%$) with the UVGI light. To achieve a given kill efficiency, the required UV irradiance I can be determined from First et al. (1999):

$$1 - \eta = \frac{N_s}{N_o} = e^{-KI\tau} \tag{6}$$

where N_s represents the number of virus particles that survived the RM3 UV-C unit; N_o the number of virus particles exposed; K the UV-C inactivation rate constant ($cm^2/\mu W \bullet s$); I the UV irradiance ($\mu W/cm^2$); and τ the exposure time (s). Buonannoet al. (2020) thought that all coronaviruses would respond similarly to the UV-C light, and thus the inactivation rate constant K for SARS-CoV-2 could refer to the K of human coronavirus 229E (HCoV-229E) or human coronavirus OC43 (HCoV-OC43).

The RM3 UV-C air disinfection unit, shown in Fig. 1(a), draws in the

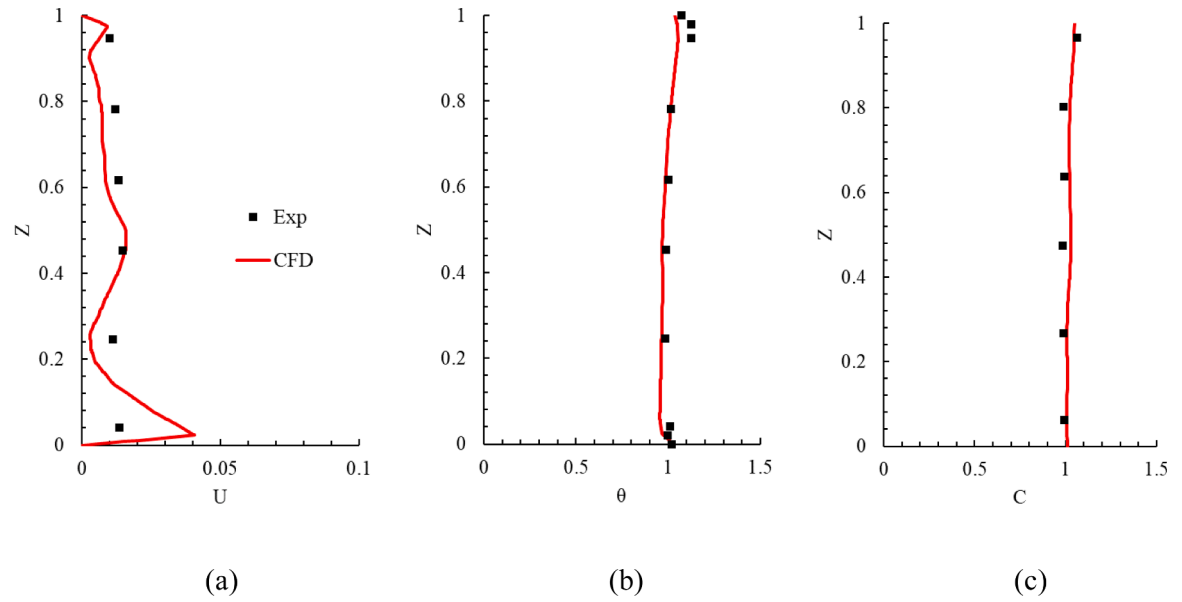

Fig. 3. Comparison of calculated results with experimental data on line 1 in the environmental chamber: (a) air velocity (b) air temperature, and (c) SF_6 concentration. In the figure, Z = measurement height/total room height of 2.43 m, U = air velocity/air supply velocity, $\theta = (T - T_{in})/(T_{out} - T_{in})$ with $T_{in} = 14.5$ °C and $T_{out} = 24.1$ °C, and $C = (c - c_{in})/(c_{out} - c_{in})$ with $c_{in} = 0.0492$ ppm and $c_{out} = 1.0496$ ppm.

surrounding air at the base and discharges treated air at the top. The height of RM3 UV-C unit is 2.29 m (7.5 ft) and the diameter of the main body is 0.2 m (8 inch). It can handle 200 CFM of air with the kill efficacy of 99.9%. Fig. 1(b) depicts the simplified RM3 UV-C unit model used for the CFD simulation. Fig. 1(c) illustrates the operation of an RM3 unit when integrated with the ventilation system in an office.

The unit designed in such a way has two main advantages. One is that the unit works on the principle of a unidirectional downward flow as shown in Fig. 1(b), thus it can exert a downward push on the microdroplets to force them to drop to the floor before landing on surfaces or being inhaled by occupants. Another one is that it can prevents stirring up of microdroplets that have dropped to the floor level. Compared with the displacement ventilation system (Kong et al., 2021) with higher contamination discharge efficiency, the RM3 UV-C air disinfection unit design is most effective in a well-mixed ventilation configuration.

Since the shortwave UV-C in the RM3 unit can effectively eradicate the pathogens in the return air, it can inhibit the transmission of airborne diseases to occupants in close proximity in the office space. Thus, the 6-feet social distancing rule (Feng et al., 2020) could be reduced in indoor environments.

3. Results

This section describes our validation of the CFD simulation results and our use of the CFD tool to study the performance of ventilation systems and RM3 UV-C units in buildings.

3.1. CFD validation

This investigation validated the CFD simulations by comparing the numerical results with measured data from Srebric and Chen (2002), where flow characteristics were typical for office buildings. The experiment was conducted in a full-scale environmental chamber, as shown in Fig. 2, with a mixing ventilation system. The dimensions of the chamber were 5.16 m × 3.65 m × 2.43 m. Outdoor air was supplied through a square diffuser installed in the ceiling and exhausted through an outlet near the floor at a ventilation rate of 4.9 ACH. The air supply velocity and temperature were 5.2 m/s and 14.5 °C, respectively. The temperature of the wall, floor, ceiling, and window were 24 °C, 24.23 °C, 24.32 °C, 26.95 °C, respectively. The occupants (74 W), computer 1 (108 W), computer 2 (173 W), and lights (34 W) were constant heat sources that included radiation and convection. In addition, this study assumed that convective heat transfer accounted for 60% and was used to set the heat flux boundary conditions. Other detailed geometry information is available from Srebric and Chen (2002). In this investigation, the environmental chamber model was discretized by about 4.3 million non-uniform triangular pyramid cells, with which this study achieved grid-independent results. Three black lines in Fig. 2 represent the measurement locations.

Fig. 3 compares the measured and calculated results in the environmental chamber. The results are presented only for line 1 because the results on the other lines were similar (the results on lines 2 and 3 can be found in Appendix A section). Since there were some uncertainties in the measurement of low air velocity and because there were numerical errors in the simulated results, it was difficult to achieve perfect agreement between the experimental data and numerical results. The predicted results shown in Fig. 3 were acceptable for our applications, and thus this study could use the CFD tool to simulate the airflow, air temperature, and SARS-CoV-2 quanta concentration in office buildings with the expectation of reliable results.

3.2. Ventilation and air disinfection system study

Most office buildings in the United States use conventional well-mixed ventilation systems, which dilute contaminated air with supply air to achieve an acceptable, uniform contaminant concentration. Many offices use recirculated air that is filtered by conventional, low-grade filters (primary filters) and these primary filters mainly for filtration particles above 5 μm. Such filters have close to 0% filtration efficiency for the SARS-CoV-2 virus which is usually less than 5 μm. The problem could be remedied with the use of auxiliary air disinfection devices.

This study used RM3 units together with a mixing ventilation system for a one-floor building with a combination of individual offices and workstations as shown in Fig. 4(a). The dimensions of each office were 47.2 m × 14.3 m × 5.6 m. The doors to the individual offices were closed, and a 3 cm gap between the floor and the lower door frame allowed air exchange between the individual offices and the larger space with workstations. This study used actual information measured at diffusers as inputs. The flow rate of outdoor air through the ventilation system was 946 m^3/h or 0.46 ACH, which accounted for only 10% of the

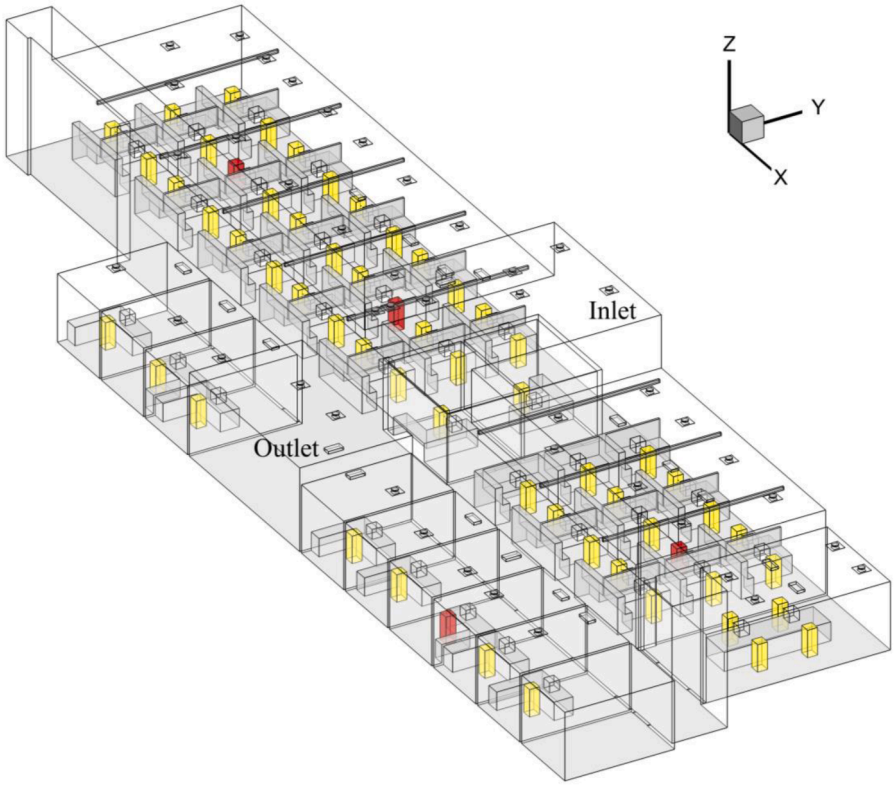

(a) Layout of the office building

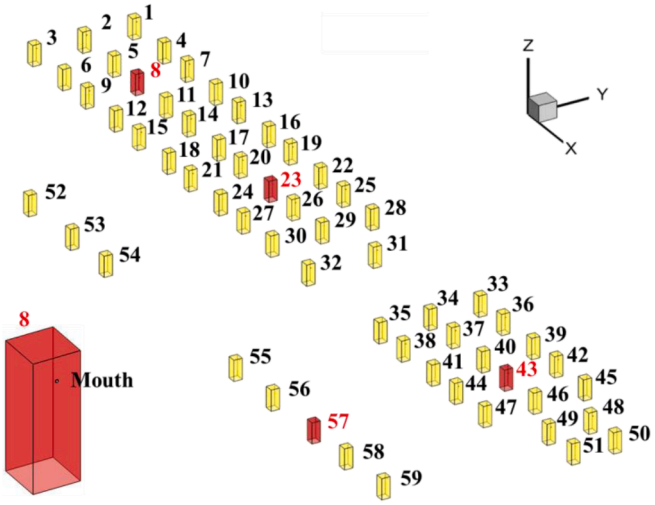

(b) Locations of the 59 people in the offices, with four index patients shown in red

Fig. 4. The office building and its occupant distribution.

total ventilation rate (9460 m^3/h). The remaining 90% was recirculated air. As depicted in Fig. 4(b), the office had a total of 59 occupants, and the 4 occupants shown in red were assumed to be COVID-19 patients. The viruses were released through the patients' mouth, as shown in Fig. 4(b), and the breathing rate and quanta value were 0.3 m^3/h and 31 h^{-1}, respectively. Each person had a desktop computer. The temperature boundary conditions of the supplied air, the computer and the occupants were 21.11 °C (70 ℉), 32.22 °C (90 ℉) and 31.11 °C (88 ℉), respectively. The CFD simulations used more than 20 million cells to achieve grid-independent solutions.

To reduce the infection risk in the office, this study proposed the installation of thirty-six RM3 UV-C units with disinfection efficiency of 99.9%. For each unit, the flow rate was 339.8 m^3/h. The units supplied a total of 12,221 m^3/h (= 36 units × 339.8 m^3/(h•unit) × 0.999) clean air to the building. They were installed throughout the office as shown in Fig. 5.

To evaluate the performance of the RM3 UV-C units and assess whether the existing ventilation system provided sufficient outdoor air, this study used the existing system without RM3 units as the reference case (or Case A in Table 1). Case B was the same as Case A but with 100%

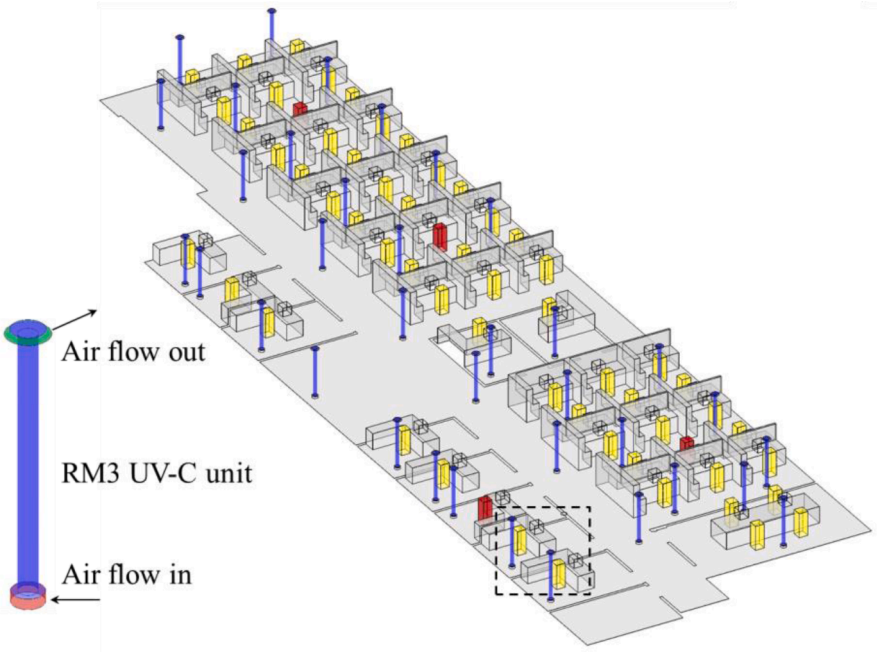

(a) Distribution of the 36 RM3 UV-C units in the office building

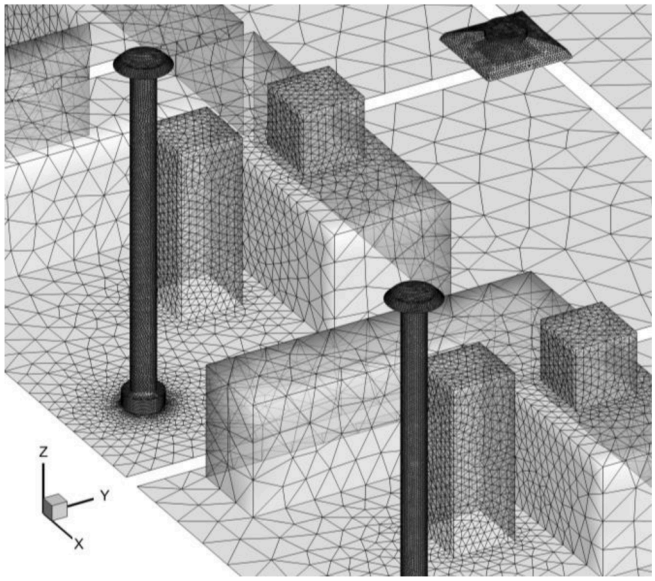

(b) mesh information of the black dashed area in the upper figure

Fig. 5. Distribution of the 36 RM3 UV-C units in the office building and mesh information.

Table 1
Key information for the four cases used in this study.

Case	Outdoor air (m^3/h)	Recirculated air	Filtration efficiency	Cleaning device	Treated air flow rate (m^3/h)	Disinfection efficiency	Equivalent ventilation rate (ACH)
A	946	90%	0	None	–	–	0.46
B	9460	0%	0	None	–	–	4.55
C	946	90%	0	RM3	12,221	99.9%	6.33
D	9460	0%	0	RM3	12,221	99.9%	10.43

outside air. Case C was the same as Case A but with 36 RM3 units that had a 99.9% disinfection efficiency for SARS-CoV-2. Case D was the same as Case B but with 36 RM3 units, or the same as Case C but with 100% outdoor supply air. Table 1 provides the technical specifications of the four cases used in this study. Note that the equivalent ventilation rate is equal to the sum of the outdoor air flow rate and the flow rate of

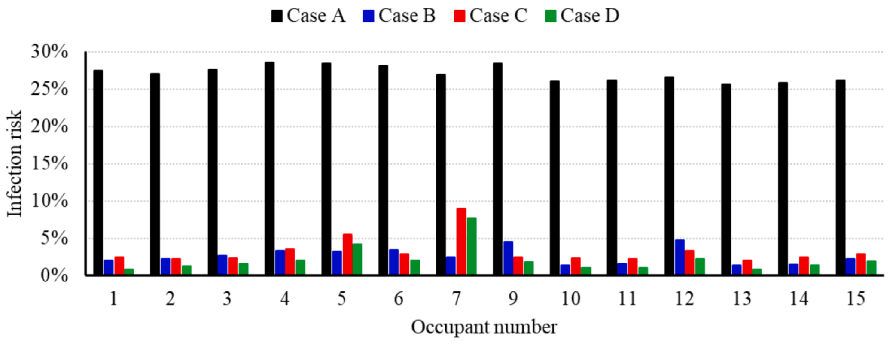

(a) Occupants 1-15

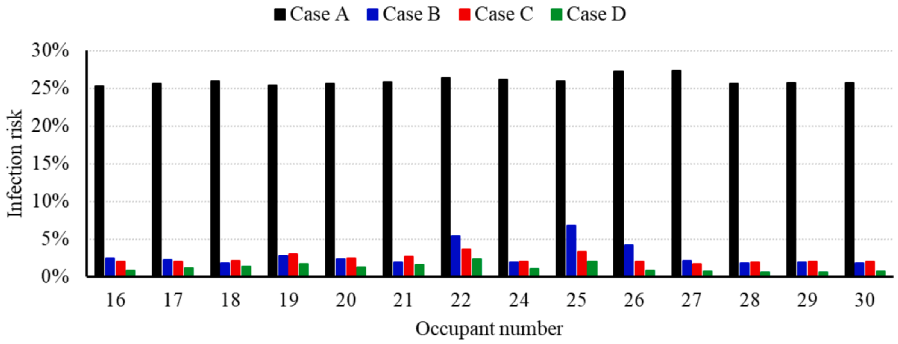

(b) Occupants 16-30

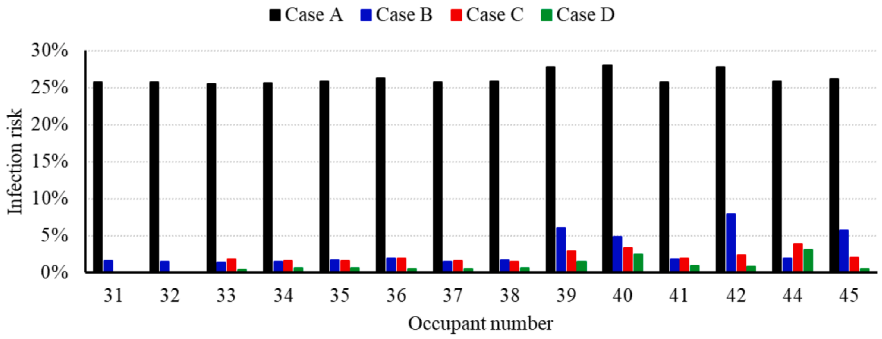

(c) Occupants 31-45

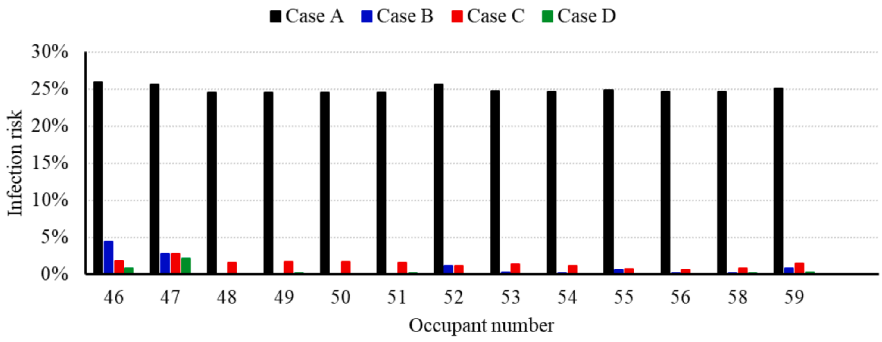

(d) Occupants 46-59

Fig. 6. The infection risk probability for each susceptible occupant in different cases (Detail results can be found in Appendix B). (For interpretation of the references to color in this figure, the reader is referred to the web version of this article).

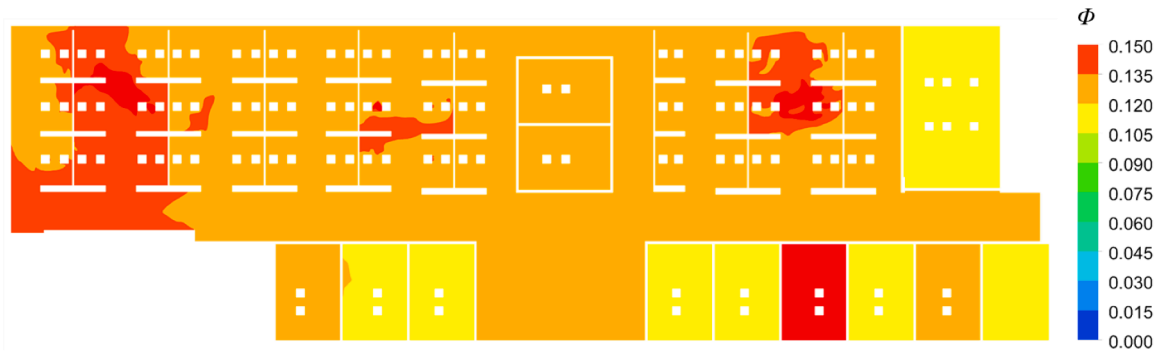

(a) Quanta concentration distribution

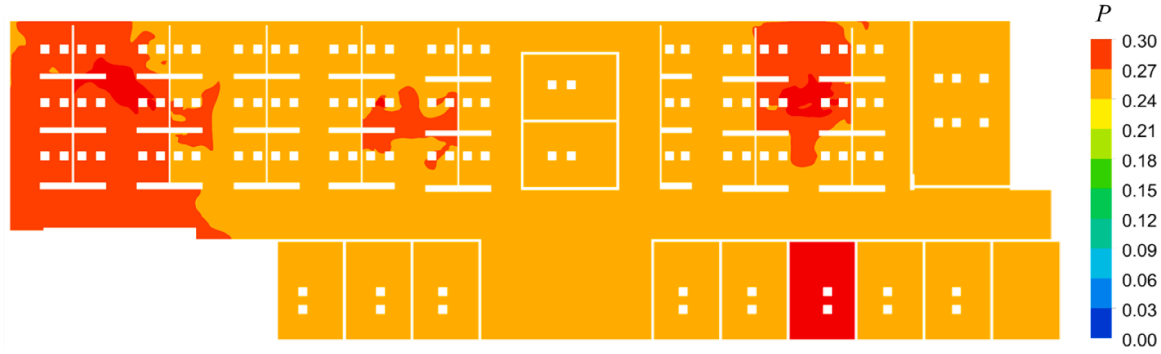

(b) Infection risk distribution

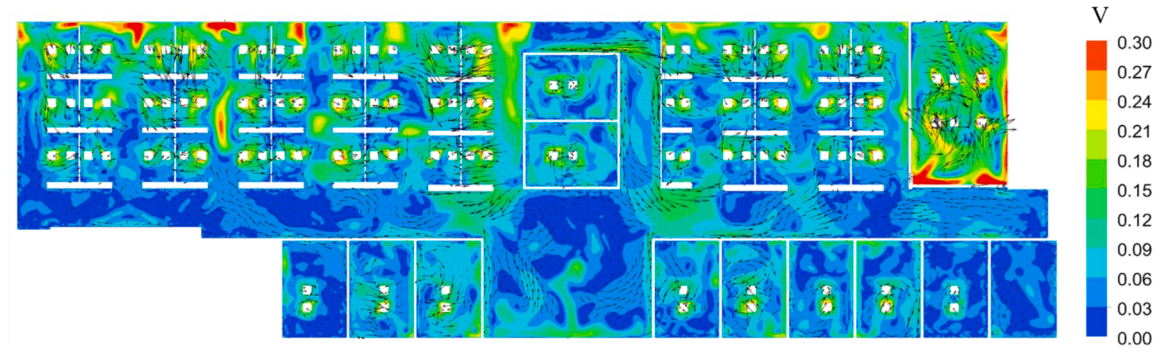

(c) Air velocity distribution

Fig. 7. Distribution of quanta concentration, infection risk, air velocity in the beathing zone ($Z = 1.1$ m) in Case A.

air treated by the RM3 UV-C units divided by the volume of the office building.

The average infection risk probability and quanta concentration calculated by Eqs. (2) and (3) for Case A were 26.99% and 0.13 per m^3, respectively, for an eight-hour stay in the office. The black histograms in Fig. 6 portray the infection risk probability for each susceptible occupant, obtained by means of Eq. (5). Due to the well-mixed ventilation system, the infection risk for the susceptible occupants was close to the average value. Occupants 1–6, 9, 26, 27, 38, 39, 40, and 42 had a higher infection probability than others, because these people were in close proximity to infected occupants 8, 23, and 43.

Next, Fig. 7(a) displays the quanta concentration in the breathing zone (at a height of 1.1 m from the floor). Note that, the average value was 0.13 per m^3. The results indicate that the quanta concentration was higher near the index patients than in other areas. In the individual offices, where there were outlets, the quanta concentration was lower than the average value. Fig. 7(b) and (c) display the distribution of the infection risk and air velocity vectors in the breathing zone, respectively. Since the indoor air flow is evenly mixed, the infection probability in the breathing zone is near the average value (27%).

With the higher outdoor air ventilation rate in Case B, the average infection risk was sharply reduced to only 3.10% for an 8 h stay. The corresponding average quanta concentration for Case B was 0.013 per m^3. Note that, since the difference between Case B and Case A is the outdoor air ratio, the flow field of Case B is exactly the same as that of Case A as shown in Fig. 7(c).

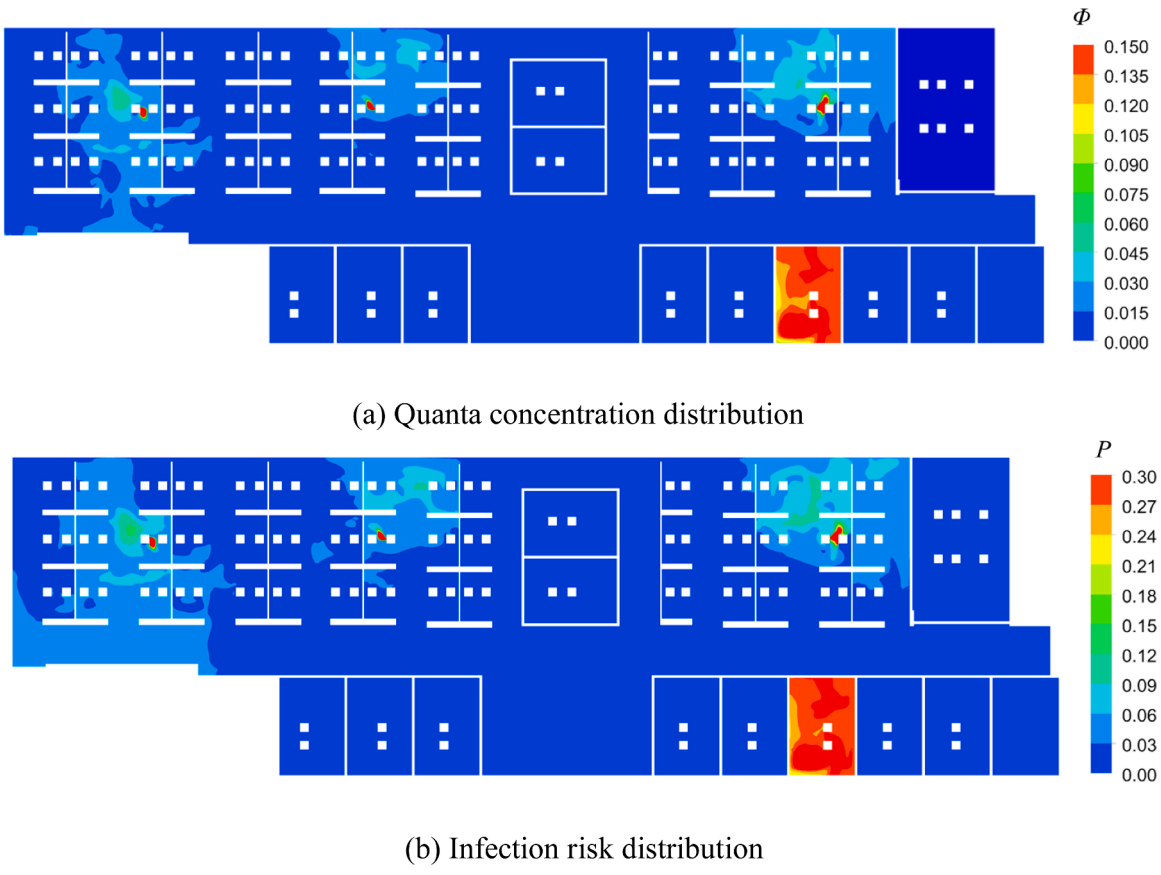

Fig. 8. Distribution of quanta concentration and infection risk in the breathing zone ($Z = 1.1$ m) in Case B.

The blue histograms in Fig. 6 indicate the infection risk for each susceptible person. Among the occupants of the individual offices (31, 32, 48–56, 58, 59), the infection risk for the majority (48–56, 58, 59) was reduced to almost 0%. The infection risk for occupants 31 and 32 was 1.58% and 1.50%, respectively, because their offices did not have any air supply diffusers or outlets, and the indoor air could be exchanged only through the gap between the floor and the door frame.

Meanwhile, Fig. 8 depicts the areas in which quanta concentration and infection risk distribution. A comparison of Figs. 7 and 8 reveals that the area that above the average value (0.013 per m^3 and 3.1%) for Case B was similar to that for Case A. The uniform distribution of the outlets prevented excessive accumulation of the quanta in some areas.

Compared with Case A (26.99%), the 36 RM3 UV-C units used in Case C (2.23%) reduced the average infection risk probability by 24.74%. In addition, the average infection risk P_C (2.23%) was smaller than P_B (3.10%), which occurred because the amount of outdoor air (9460 m^3/h) used in Case B was smaller than the amount of equivalent clean air (946 + 12,221 = 13,167 m^3/h) used in Case C. Note that the infection risk difference among the susceptible occupants, as depicted by the red histograms in Fig. 6, was much smaller than that in Case B, because the RM3 UV-C units were almost evenly distributed in the building. The distribution of quanta concentration, infection risk, air velocity in Case C is displayed in Fig. 9. A comparison of Figs. 7 and 9 indicates that RM3 UV-C units can decrease the quanta concentration and infection risk obviously. Note that, with higher amount of recirculation air, the air velocity as shown in Fig. 9(c) is higher than Fig. 7(c).

Ideally, buildings with an infection risk of lower than 2% (Sun & Zhai, 2020) would be a better indoor environment for people to return to the workplace during the epidemic. Cases B and C were still above the threshold. Therefore, this investigation used 100% outdoor air and 36 RM3 UV-C units simultaneously in Case D. This effort reduced the average infection risk probability and quanta concentration in the office to be only 1.36% and 0.00575 per m^3, respectively. The infection risk for each susceptible person in Case D is depicted by the green histograms in Fig. 6. Although the distribution of the RM3 UV-C units was fairly uniform, occupants benefited differently due to the non-even distribution of the air supply diffusers, local air patterns, and proximity to the index patients. Fig. 10 shows the quanta concentration and infection risk distribution in the breathing zone. This figure also clearly demonstrates that the occupants located near the index patients were exposed to a high quanta concentration and infection risk.

Fig. 11 compares the average infection risk in the four cases. When the amount of equivalent clean air indoors was low, increasing the clean air supply (Case B) or using RM3 UV-C units (Case C) would significantly reduce the infection risk. An infection risk below 2% (Sun & Zhai, 2020) would require the use of 100% outdoor air and the RM3 units together. The use of 100% outdoor air would significantly increase the energy costs for air handling and employing RM3 UV-C units could be preferrable. In Case C, where the infection probability was close to 2%, additional RM3 units could be used to reduce the probability below 2% while still using minimal outdoor air as in the current design.

4. Discussion

Since the office building was very large, the use of a model with realistic human geometry for the occupants would have dramatically increased the number of computer cells required. Therefore, this investigation used a rectangular column to represent an occupant. Cheng and Lin (2016)) studied different geometries for the human body and found the simplified rectangular model to be satisfactory.

The quanta value provided by Dai and Zhao (2020) was based on previous data. As the COVID-19 epidemic continues, future studies can assess the infection risk based on the latest quanta value using the same method.

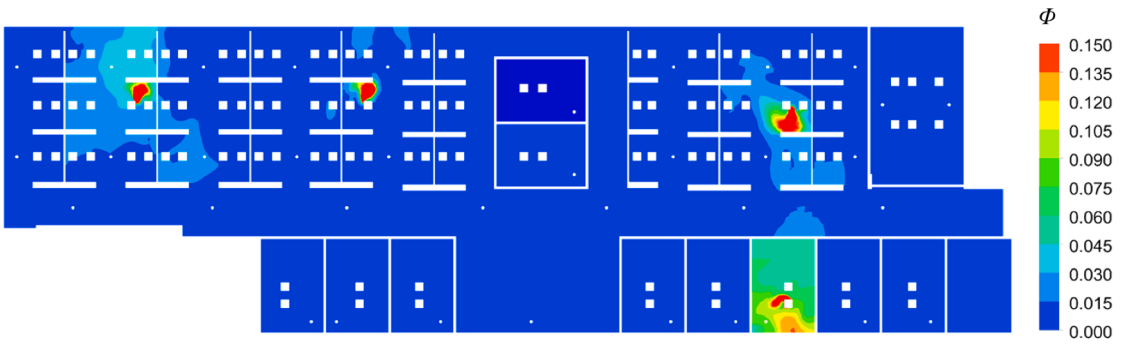

(a) Quanta concentration distribution

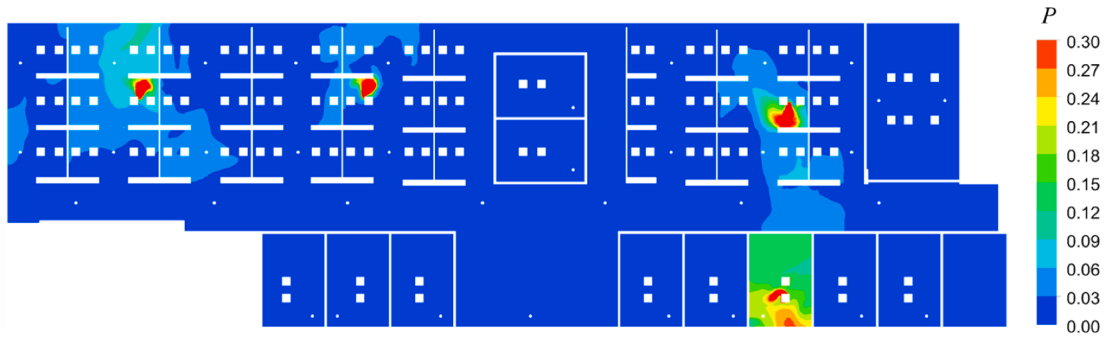

(b) Infection risk distribution

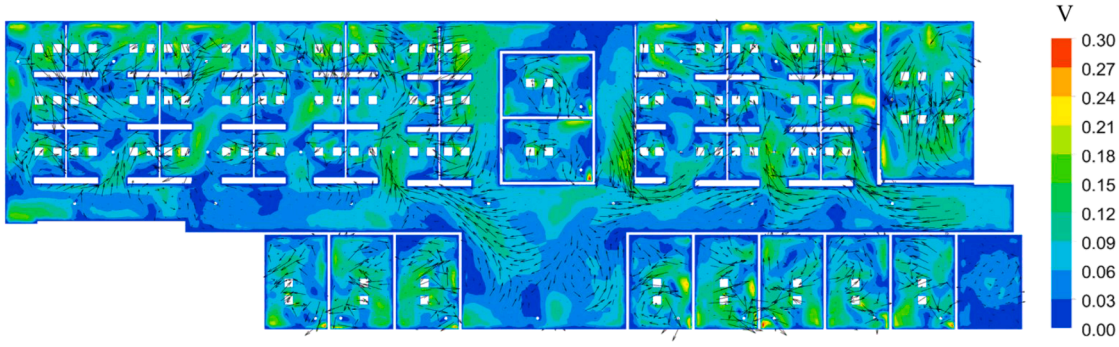

(c) Air velocity distribution

Fig. 9. Distribution of quanta concentration, infection risk, air velocity in the beathing zone ($Z = 1.1$ m) in Case C.

RM3 UV-C units developed in this study only handle the indoor air using the UVGI light and then send back into the room. Since the RM3 UV-C units do not need extra energy to heat, cool or (de)humidify the indoor air (Sha et al., 2021), it can achieve lowers investment and operational costs.

The RM3 UV-C units as shown in Fig. (1) draws the air from the bottom and discharges the treated air from the top. However, it would be worse for the indoor comfort and indoor air quality when the treated air discharged from the bottom. That was because it may raise the settled virus again which would pollute the air in the breathing zone and cause draft sensation.

Since it is too difficult to conduct the experiment using the SARS-CoV-2 virus, this investigation did not directly measure the kill efficiency of RM3 UV-C units by experiment but designed the RM3 UV-C units according to the research results of Narita et al. (2020) and the calculation formula as shown in Eq. (6) from First et al. (1999). The proposed RM3 UV-C unit was designed with a 99.9% kill efficiency by the utilizing optimum powered UV-C lights in the assembly. In addition, the effectiveness of RM3 is mostly affected by the air filter, the filter may get clogged up and lesser air would be drawn in after prolonged use. It will certainly lower the effectiveness of the RM3 UV-C units, so it is necessary to clean the filter regularly.

The methodology used to evaluate the infection risk in the office building was based on the steady state assumption, however, unsteady boundary conditions and the movement of the occupants would form unsteady flow filed which may further affect the transmission of the SARS-CoV-2 virus. Future study would explore the transmission of the SARS-CoV-2 virus under the unsteady state.

In this study, four infected persons were evenly and randomly distributed to study the probability of infection. For real cases, the locations of the infected people need to be determined according to the actual situation.

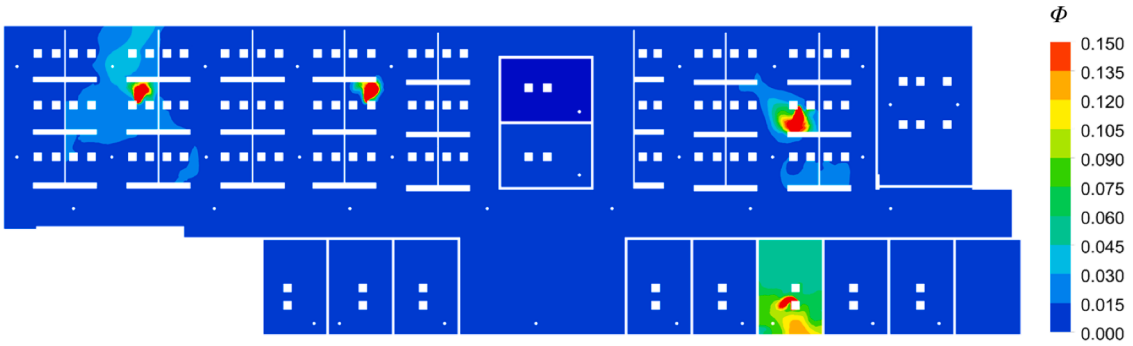

(a) Quanta concentration distribution

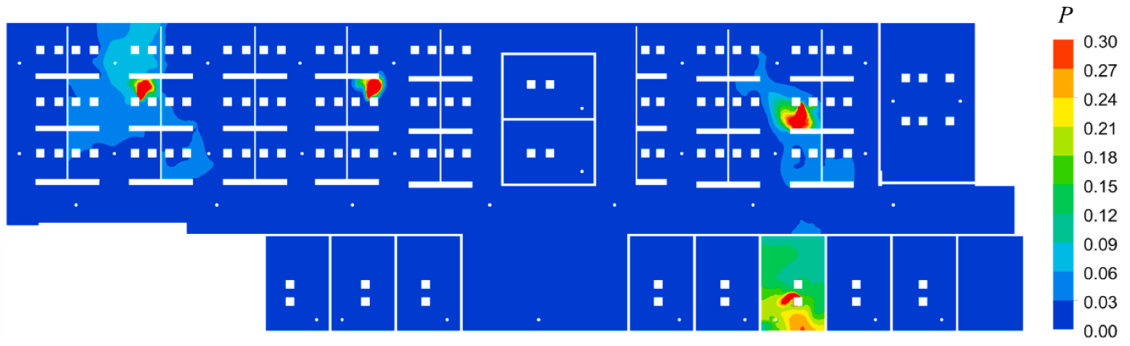

(b) Infection risk distribution

Fig. 10. Distribution of quanta concentration and infection risk in the beathing zone (Z = 1.1 m) in Case D.

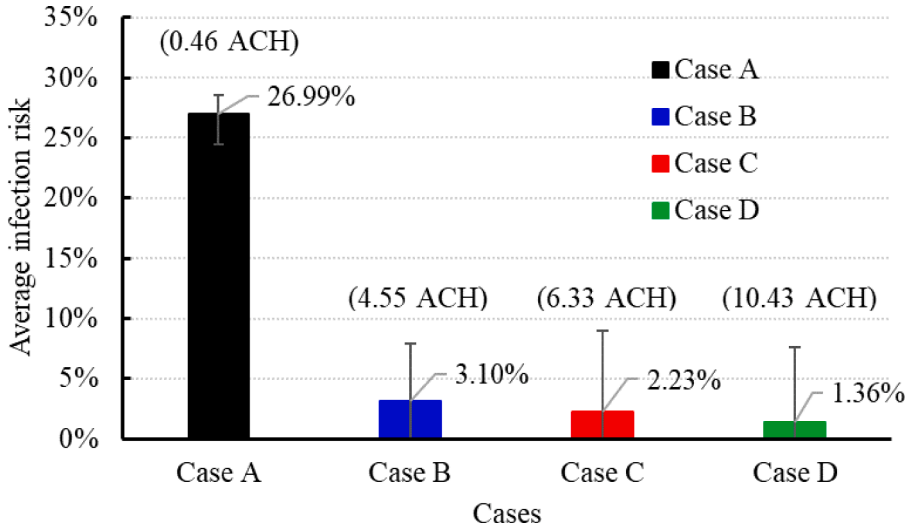

Fig. 11. Average infection risk in the four cases.

This investigation added one more case, Rheem office with 49 occupants, as shown in Fig. 12(a) for comparison. The geometry and number of the occupants were different with Roswell office. It had the similar well-mixed ventilation system with Roswell office, while the average infection risk (20.56%) was lower than that of the Roswell office (27%). That was because the total air flow rate (946 m3/h) of the Roswell office was smaller than that of the Rheem office (12,930 m3/h). Fig. 12(b) shows the infection risk distribution which indicated that the infection risk in the office near the average value except the area around the index patients. All in all, whether it is Roswell office or Rheem office, the infection risk mainly depends on the amount of clean air.

For the studied Roswell office example, this investigation used 36 RM3 UV-C units to achieve the lower infection risk. It does not mean we should install 36 RM3 UV-C units in every office building. The actual number of the RM3 UV-C units can be determined by the Eq. (2) based on the requirements. In addition, the locations of RM3 UV-C units were randomly and evenly distributed in this investigation which may not be the optimal locations. Future study would adopt the inverse design

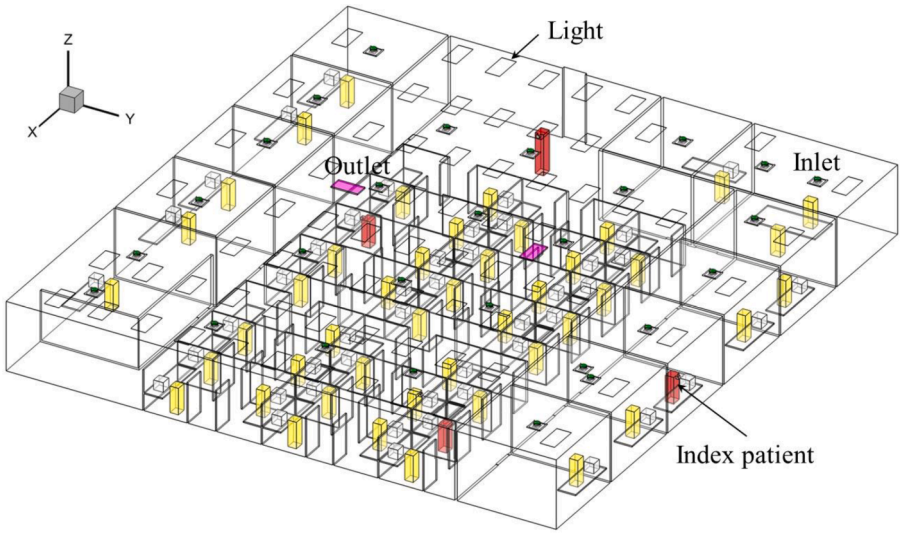

(a) Layout of the Rheem office building

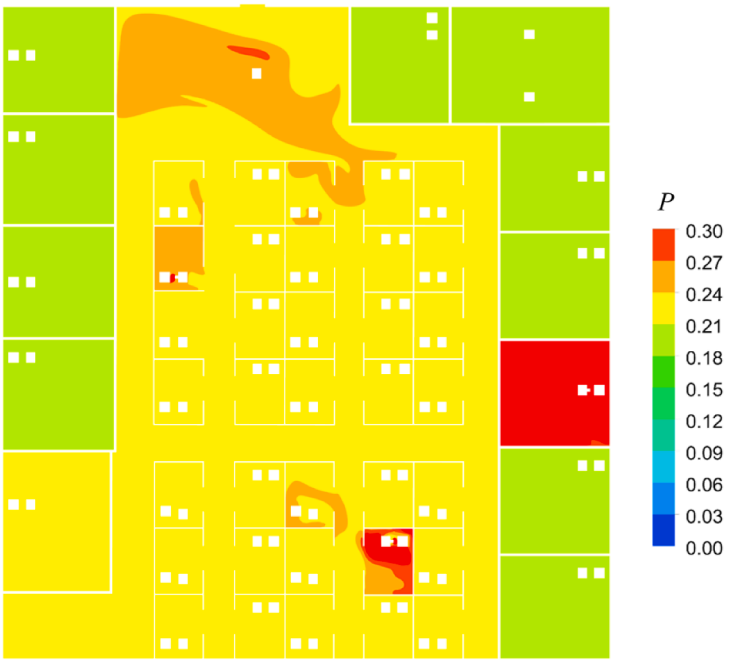

(a) Infection risk distribution

Fig. 12. Layout of the office building and distribution of infection risk in the beathing zone ($Z = 1.1$ m).

method (Zhao, Shi, & Chen, 2020, 2021) to identify the optimal locations of the RM3 UV-C units.

The communication mechanism of COVID-19 includes air transmission, contact transmission and droplet propagation. This study only explores the probability of airborne infection. Future study will investigate the deposition of virus on the surface, the risk of contact infection and droplet transmission.

Based on the above results and findings, this study would suggest that the enclosed indoor environment install air purification device or supply enough fresh air to create a healthy indoor environment and people wear surgical or N95 mask in the office to reduce the infection risk.

The simulation assumed that the efficiency of RM3 UV-C units is 99.9%, but its efficiency may decrease with the increase of service time. Therefore, the influence of this factor should be considered in practical application.

5. Conclusions

This investigation used CFD simulations and the Wells-Riley equation to assess the infection risk for susceptible people in a large office building that consisted of individual offices and a workstation area. The study compared four different ventilation/disinfection strategies: (1) with 90% recirculated air in the ventilation system, (2) with 100% outdoor air, (3) with 90% recirculated air and thirty-six RM3 UV-C units, and (4) with 100% outdoor air and thirty-six RM3 UV-C units. The

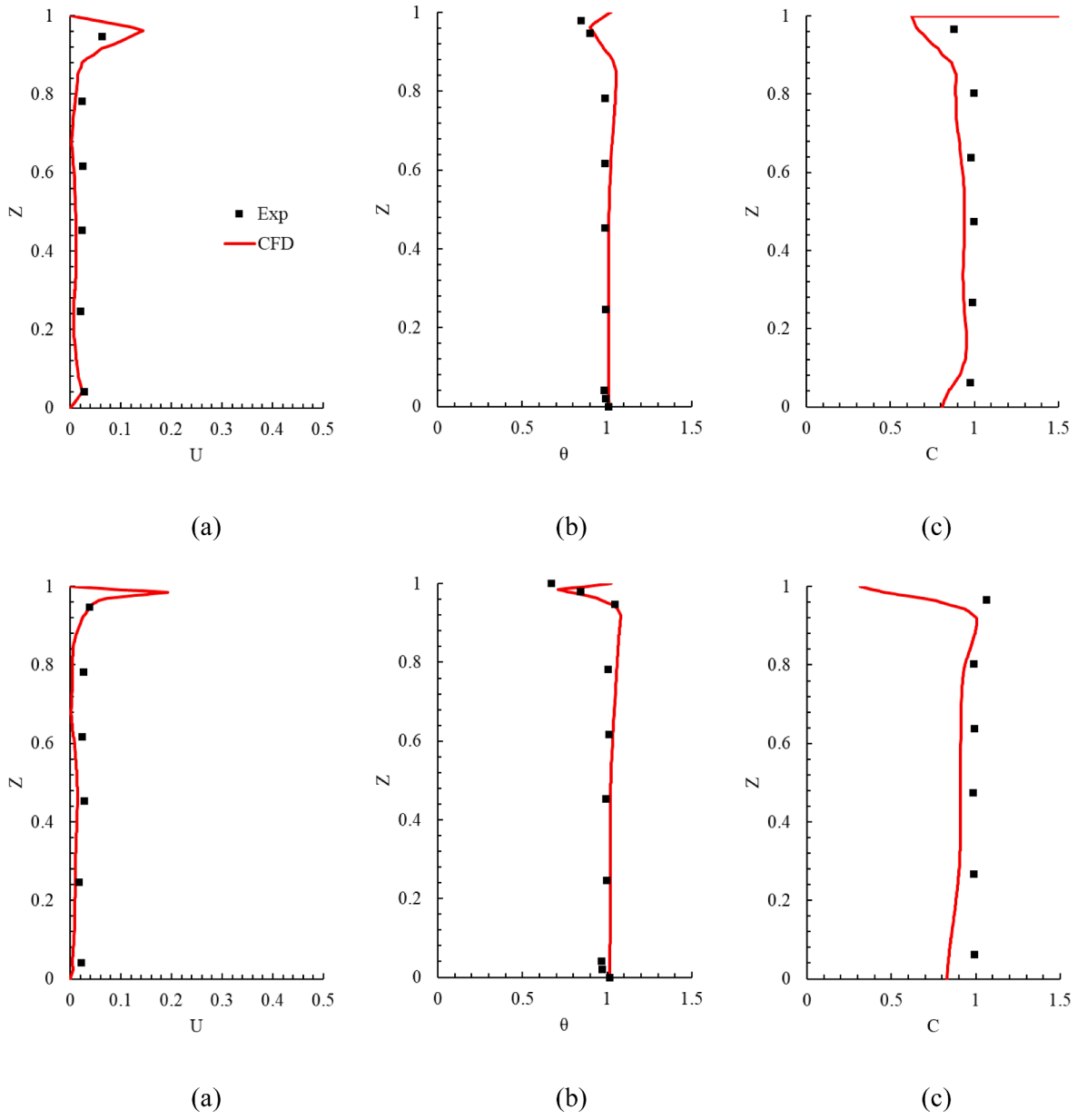

Fig. 13. Comparison of calculated results with experimental data on line 2 and 3 in the environmental chamber: (a) air velocity (b) air temperature, and (c) SF_6 concentration. In the figure, Z = measurement height/total room height of 2.43 m, U = air velocity/air supply velocity, $\theta = (T - T_{in})/(T_{out} - T_{in})$ with $T_{in} = 14.5$ °C and $T_{out} = 24.1$ °C, and $C = (c - c_{in})/(c_{out} - c_{in})$ with $c_{in} = 0.0492$ ppm and $c_{out} = 1.0496$ ppm.

following conclusions were reached:

- The use of well-mixed ventilation in the office building led to a uniform infection rate in the workstation area. Individual offices with closed doors had only a slightly lower risk because recirculated air brought the virus back to these offices. For the Roswell case of 90% recirculated air in this study, the infection risk was 27% for an 8 h stay in the office building when there were four index patients.
- The use of 100% outdoor air would reduce the infection risk sharply, but the effort would significantly increase energy costs for handling the air. The results in this study indicated that the infection risk would decrease from 27% (10% outdoor air) to only 3.1% using 100% outdoor air.
- UV-C units are highly recommended due to the minimal changes to existing ventilation systems and the minimal energy cost increase. For example, bringing the infection risk in the office below 2% which is the suggested targeted infection probability in Sun and Zhai's (2020) study would require a combination of 100% outside air and the use of the RM3 UV-C units. An alternative would be the use of more RM3 UV-C units with only 10% outside air to achieve the energy saving.
- The infection risk in well-mixed indoor environment directly depends on the amount of clean air (outside air or the treated indoor air).

Declaration of Competing Interest

With the submission of this manuscript, I would like to undertake that I have consulted the Guide for Authors in preparing my submitted manuscript. And I also acknowledge that I have prepared the manuscript in compliance with the Ethics as described in the Guide for Authors. No conflict of interest exits in the submission of this manuscript, and manuscript is approved by all authors for publication. I would like to declare on behalf of my co-authors that the work described was original

Table 2
The infection risk values of susceptible person in different cases.

Num	Case A	Case B	Case C	Case D	Num	Case A	Case B	Case C	Case D
1	27.45%	2.05%	2.45%	0.81%	31	25.68%	1.58%	0.00%	0.00%
2	27.07%	2.24%	2.24%	1.26%	32	25.72%	1.50%	0.00%	0.00%
3	27.53%	2.67%	2.32%	1.54%	33	25.50%	1.36%	1.77%	0.35%
4	28.52%	3.33%	3.59%	1.97%	34	25.57%	1.43%	1.59%	0.55%
5	28.40%	3.17%	5.45%	4.15%	35	25.85%	1.72%	1.57%	0.57%
6	28.08%	3.40%	2.84%	2.06%	36	26.23%	1.96%	1.96%	0.48%
7	26.90%	2.43%	8.97%	7.63%	37	25.70%	1.49%	1.62%	0.51%
9	28.41%	4.52%	2.45%	1.75%	38	25.80%	1.64%	1.53%	0.59%
10	26.03%	1.37%	2.36%	1.00%	39	27.76%	6.05%	2.87%	1.51%
11	26.15%	1.60%	2.28%	1.01%	40	27.96%	4.80%	3.27%	2.47%
12	26.55%	4.68%	3.31%	2.24%	41	25.70%	1.75%	1.95%	0.98%
13	25.62%	1.36%	2.05%	0.79%	42	27.74%	7.92%	2.30%	0.81%
14	25.81%	1.44%	2.43%	1.34%	44	25.85%	1.86%	3.83%	3.10%
15	26.13%	2.25%	2.85%	1.88%	45	26.14%	5.70%	1.99%	0.53%
16	25.24%	2.48%	2.04%	0.79%	46	25.89%	4.45%	1.85%	0.81%
17	25.58%	2.21%	2.01%	1.12%	47	25.59%	2.78%	2.78%	2.13%
18	25.91%	1.79%	2.11%	1.32%	48	24.50%	0.00%	1.61%	0.07%
19	25.40%	2.81%	3.02%	1.69%	49	24.50%	0.00%	1.71%	0.18%
20	25.63%	2.39%	2.43%	1.26%	50	24.50%	0.00%	1.74%	0.09%
21	25.79%	1.86%	2.64%	1.57%	51	24.50%	0.00%	1.61%	0.21%
22	26.34%	5.38%	3.64%	2.32%	52	25.55%	1.15%	1.13%	0.05%
24	26.14%	1.90%	1.99%	1.04%	53	24.72%	0.25%	1.34%	0.11%
25	25.97%	6.76%	3.29%	2.03%	54	24.63%	0.15%	1.15%	0.05%
26	27.20%	4.18%	1.98%	0.81%	55	24.89%	0.55%	0.75%	0.04%
27	27.32%	2.13%	1.68%	0.67%	56	24.60%	0.12%	0.65%	0.02%
28	25.65%	1.79%	1.90%	0.58%	58	24.61%	0.16%	0.82%	0.21%
29	25.72%	1.87%	1.98%	0.62%	59	25.11%	0.78%	1.47%	0.23%
30	25.76%	1.85%	2.00%	0.67%					

research that has not been published previously, and not under consideration for publication elsewhere, in whole or in part. All the authors have approved the manuscript that is enclosed.

Acknowledgment

This work was partially supported by Jiangsu Planned Projects for Postdoctoral Research Funds through Grant No. 2021K069A (1103000286).

Appendix A. Validation results

Fig. 13

Appendix B. The infection risk values of susceptible person in different cases

Table 2

References

Agarwal, N., Meena, C. S., Raj, B. P., Saini, L., Kumar, A., Gopalakrishnan, N., et al. (2021). Indoor air quality improvement in COVID-19 pandemic: Review. *Sustainable Cities and Society, 70*, Article 102942.

American Society of Heating. (2019). Refrigerating and air-conditioning engineers (ASHRAE) ventilation for acceptable indoor air quality: 62 (p. 1). Atlanta, USA: ASHRAE Standard.

ANSYS. (2010). Fluent 12.1 documentation. Lebanon, NH: Fluent Inc.

ASHRAE (2020). ASHRAE issues statements on relationship between COVID-19 and HVAC in buildings, (2020). https://www.ashrae.org/about/news/2020/ashrae-issues-statements-on-relationship-between-covid-19-and-hvac-in-buildings. Retrieved on 22 October 2020.

Blocken, B., Druenen, T. V., Ricci, A., Kang, L., & Brombacher, A. C. (2021). Ventilation and air cleaning to limit aerosol concentrations in a gym during the COVID-19 pandemic. *Building and Environment, 193*(9), Article 107659.

Boussinesq, J. (1903). *Theorie analytique de la chaleur*. Gauthier-Villars.

Buonanno, M., Ponnaiya, B., Welch, D., Stanislauskas, M., Ransders-Pehrson, G., Smilenov, L., et al. (2017). Germicidal efficacy and mammalian skin safety of 222-nm UV light. *Radiation Research, 187*(4), 493–501.

Buonanno, M., Welch, D., Shurak, I., & Brenner, D. J. (2020). Far-UVC light (222nm) efficiently and safely inactivates airborne human coronaviruses. *Scientific Reports, 10*, 10285.

Cao, S. J. (2018). Challenges of using CFD simulation for the design and online control of ventilation systems. *Indoor and Built Environment, 28*(1), 3–6.

Cao, S. J., Yu, C. W., & Luo, X. (2020). Heating, ventilating and air conditioning system and environmental control for wellbeing. *Indoor and Built Environment, 29*(9), 1191–1194.

Casini, B., Tuvo, B., Cristina, M. L., et al. (2019). Evaluation of an ultraviolet C (UVC) light-emitting device for disinfection of high touch surfaces in hospital critical areas. *International Journal of Environmental Research and Public Health, 16*(19), 3572.

CDC. (2020). *SARS-CoV-2 & potential airborne transmission*. Centers for Disease Control and Prevention. https://www.cdc.gov/coronavirus/2019-ncov/more/scientific-brief-sars-cov-2.html. Retrieved on 21 October 2020.

Chen, H., Zhou, X., Feng, Z., & Cao, S. J. (2021). Application of polyhedral meshing strategy in indoor environment simulation: Model accuracy and computing time. *Indoor and Built Environment*.

Chen, Q. (1995). Comparison of different k-ε models for indoor air flow computations. *Numerical Heat Transfer, Part B: Fundamentals, 28*, 353–369.

Cheng, Y., & Lin, Z. (2016). Experimental investigation into the interaction between the human body and room airflow and its effect on thermal comfort under stratum ventilation. *Indoor air, 26*(2), 274–285.

Choudhury, D. (1993). *Introduction to the renormalization group method and turbulence modeling, Canonsburg*. Fluent Inc. Technical Memorandum TM-107.

Crema, E. (2021). The SARS-COV-2 outbreak around the Amazon rainforest: The relevance of the airborne transmission. *The Science of the Total Environment, 759*, Article 144312.

Dai, H., & Zhao, B. (2020). Association of the infection probability of COVID-19 with ventilation rates in confined spaces. *Building Simulation, 13*, 1321–1327.

Ding, J., Yu, C. W., & Cao, S. J. (2020). HVAC systems for environmental control to minimize the COVID-19 infection. *Indoor and Built Environment, 29*(9), 1195–1201.

Doremalen, N. V., Bushmaker, T., Morris, D. H., Holbrook, M. G., & Munster, V. J. (2020). Aerosol and surface stability of SARS-CoV-2 as compared with SARS-CoV-1. *The New England Journal of Medicine, 382*(16), 1564–1567.

European Centre for Disease Prevention and Control, Heating, ventilation and air-conditioning systems in the context of COVID-19. 22 June 2020,(2020). www.ecdc.europa.eu/en/publications-data/heating-ventilation-air-conditioning-systems-covid-19. Retrieved on 22 October 2020.

Feng, Y., Marchal, T., Sperry, T., & Yi, H. (2020). Influence of wind and relative humidity on the social distancing effectiveness to prevent COVID-19 airborne transmission: A numerical study. *Journal of Aerosol Science, 147*, Article 105585.

Feng, Z., Cao, S. J., Wang, J., Kumar, P., & Haghighat, F. (2021a). Indoor airborne disinfection with electrostatic disinfector (ESD): Numerical simulations of ESD performance and reduction of computing time. *Building and Environment, 200*, Article 107956.

Feng, Z., Cao, S. J., & Haghighat, F. (2021b). Removal of SARS-CoV-2 using UV+Filter in built environment. *Sustainable Cities and Society, 74*, Article 103226.

Feng, Z. B., Yu, C. W., & Cao, S. J. (2019). Fast prediction for indoor environment: Models assessment. *Indoor and Built Environment, 28*(6), 727–730.

First, M. W., Nardell, E. A., Chaisson, W., & Riley, R. L. (1999). Guidelines for the application of upper-room ultraviolet germicidal irradiation for preventing

transmission of airborne contagion-part II: Design and operation guide. *ASHRAE Transactions, 105*(1), 877.
Guo, Y., Qian, H., Sun, Z., Cao, J., & Zhang, Y. (2021). Assessing and controlling infection risk with Wells-Riley model and spatial flow impact factor (SFIF). *Sustainable Cities and Society, 67*(17), Article 102719.
Heilingloh, C., Heilingloh, U., Schipper, L., Dittmer, U., Witzke, O., Yang, D., et al. (2020). Susceptibility of SARS-CoV-2 to UV irradiation. *American Journal of Infection Control, 48*, 1273–1275.
Kenyon, T. A., Valway, S. E., Ihle, W. W., Onorato, I. M., & Castro, K. G. (1996). Transmission of multidrug-resistant Mycobacterium tuberculosis during a long airplane flight. *New England Journal of Medicine, 334*(15), 933–938.
Klepeis, N. E., Nelson, W. C., Ott, W. R., Robinson, J. P., Tsang, A. M., Switzer, P., et al. (2001). The National Human Activity Pattern Survey (NHAPS): A resource for assessing exposure to environmental pollutants. *Journal of Exposure Science and Environmental Epidemiology, 11*(3), 231–252.
Kong, X., Guo, C., Lin, Z., Duan, S., He, J., Ren, Y., et al. (2021). Experimental study on the control effect of different ventilation systems on fine particles in a simulated hospital ward. *Sustainable Cities and Society, 73*, Article 103102.
Li, Y., Leung, G. M., Tang, J. W., Yang, X., Chao, C. Y. H., Lin, J. Z., et al. (2007). Role of ventilation in airborne transmission of infectious agents in the built environment-A multidisciplinary systematic review. *Indoor Air, 17*(1), 2–18.
Li, Y., Qian, H., Hang, J., Chen, X., & Kang, M. (2021). Probable airborne transmission of SARSs-CoV-2 in a poorly ventilated restaurant. *Building and Environment, 196*(5), Article 107788.
Liu, Y., Ning, Z., Chen, Y., Guo, M., Liu, Y., Gali, N. K., et al. (2020). Aerodynamic analysis of SARS-CoV-2 in two Wuhan hospitals. *Nature, 582*, 557–560. https://www.nature.com/articles/s41586-020-2271-3.
Liu, Z., Li, R., Wu, Y., Ju, R., & Gao, N. (2021). Numerical study on the effect of diner divider on the airborne transmission of diseases in canteens. *Energy and Buildings, 248*(9), 111171.
Man, P., Paltansing, S., Ong, D. S. Y., Vaessen, N., Nielen, G., & Koeleman, J. G. M. (2020). Outbreak of coronavirus disease 2019 (COVID-19) in a nursing home associated with aerosol transmission as a result of inadequate ventilation. *Clinical Infectious Diseases*. https://doi.org/10.1093/cid/ciaa1270
Melikov, A. K., Ai, Z. T., & Markov, D. G. (2020). Intermittent occupancy combined with ventilation: An efficient strategy for the reduction of airborne transmission indoors. *Science of The Total Environment, 744*, Article 140908.
Mo, J., Tian, E., & Pan, J. (2020). New electrostatic precipitator with dielectric coatings to efficiently and safely remove sub-micro particles in the building environment. *Sustainable Cities and Society, 55*, Article 102063.
Morawska, L., & Cao, J. (2020). Airborne transmission of SARS-CoV-2: The world should face the reality. *Environment International, 139*, Article 105730.
Morawska, L., & Milton, D. K. (2020). It is time to address airborne transmission of coronavirus disease 2019 (COVID-19). *Clinical Infectious Diseases, 71*, 2311–2313.
Moser, M. R., Bender, T. R., Margolis, H. S., Noble, G. R., Kendal, A. P., & Ritter, D. G. (1979). An outbreak of influenza aboard a commercial airliner. *American Journal of Epidemiology, 110*(1), 1–6.
Nakpan, W., Yermakov, M., Indugula, R., Reponen, T., & Grinshpun, S. (2019). Inactivation of bacterial and fungal spores by UV irradiation and gaseous iodine treatment applied to air handling filters. *Science of the Total Environment, 671*, 59–65.
Narita, K., Asano, K., Naito, K., Ohashi, H., Sasaki, M., Morimoto, Y., et al. (2020). Ultraviolet C light with wavelength of 222nm inactivates a wide spectrum of microbial pathogens. *Journal of Hospital Infection, 105*(3), 459–467.
Olsen, S. J., Chang, H. L., Cheung, T. Y. Y., Tang, A. F. Y., Fisk, T. L., Ooi, S. P. L., et al. (2003). Transmission of the severe acute respiratory syndrome on aircraft. *New England Journal of Medicine, 349*(25), 2416–2422.
Patankar, S. V., & Spalding, D. B. (1972). A calculation procedure for heat, mass and momentum transfer in three-dimensional parabolic flows. *International Journal of Heat and Mass Transfer, 15*(10), 1787–1806.
Pei, G., Taylor, M., & Rim, D. (2021). Human exposure to respiratory aerosols in a ventilated room: Effects of ventilation condition, emission mode, and social distancing. *Sustainable Cities and Society, 73*, Article 103090.
Rahmani, A. M., & Mirmahaleh, S. Y. H. (2021). Coronavirus disease (COVID-19) prevention and treatment methods and effective parameters: A systematic literature review. *Sustainable Cities and Society, 64*, Article 102568.
Rahmani, A. R., Leili, M., Azarian, G., & Poormohammadi, A. (2020). Sampling and detection of corona viruses in air: A mini review. *The Science of the Total Environment, 740*, Article 140207.
Ren, C., & Cao, S. J. (2020). Implementation and visualization of artificial intelligent ventilation control system using fast prediction models and limited monitoring data. *Sustainable Cities and Society, 52*, Article 101860.
Ren, C., & Cao, S. J. (2021). Construction of linear temperature model using non-dimensional heat exchange ratio: Towards fast prediction of indoor temperature and heating, ventilation and air conditioning systems control. *Energy and Buildings, 251*, Article 111351.
Ren, C., Chang, X., Wang, J., Feng, Z., Nasiri, F., Cao, S. J., et al. (2021). Mitigating COVID-19 infection disease transmission in indoor environment using physical barriers. *Sustainable Cities and Society, 74*, Article 103175.
Riley, E. C., Murphy, G., & Riley, R. L. (1978). Airborne spread of measles in a suburban elementary school. *American Journal of Epidemiology, 107*, 421–432.
Sha, H., Xin, Z., & Qi, D. (2021). *Optimal control of high-rise building mechanical ventilation system for achieving low risk of COVID-19 transmission and ventilative cooling*. Sustainable Cities and Society, Article 103256.
Shi, Z., Lu, Z., & Chen, Q. (2019). Indoor airflow and contaminant transport in a room with coupled displacement ventilation and passive-chilled-beam systems. *Building and Environment, 161*, Article 106244.
Srebric, J., & Chen, Q. (2002). Simplified numerical models for complex air supply diffusers. *HVAC&R Research, 8*(3), 277–294.
Sun, C., & Zhai, J. Z. (2020). The efficacy of social distance and ventilation effectiveness in preventing COVID-19 transmission. *Sustainable Cities and Society, 62*, Article 102390.
To, G., & Chao, C. (2009). Review and comparison between the Wells-Riley and dose-response approaches to risk assessment of infectious respiratory diseases. *Indoor Air, 20*(1), 2–16.
Wang, J., Huang, J., Feng, Z., Cao, S. J., & Haghighat, F. (2021). Occupant-density-detection based energy efficient ventilation system: Prevention of infection transmission. *Energy and Buildings, 240*(5), Article 110883.
Wells, W. F. (1955). *Airborne contagion and air hygiene* (pp. 117–122). Cambridge University Press.
Xu, C., Luo, X., Yu, C., & Cao, S. J. (2020). The 2019-nCoV epidemic control strategies and future challenges of building healthy smart cities. *Indoor and Built Environment, 29*(5), 639–644.
Yao, M., Zhang, L., Ma, J., & Zhou, L. (2020). On airborne transmission and control of SARS-Cov-2. *The Science of the Total Environment, 731*, Article 139178.
You, R., Lin, C. H., Wei, D., & Chen, Q. (2019). Evaluating the commercial airliner cabin environment with different air distribution systems. *Indoor Air, 29*, 840–853.
Zhang, S., Ai, Z., & Lin, Z. (2020). Occupancy-aided ventilation for both airborne infection risk control and work productivity. *Building and Environment, 188*, Article 107506.
Zhang, Z., & Chen, Q. (2007). Comparison of the Eulerian and Lagrangian methods for predicting particle transport in enclosed spaces. *Atmospheric Environment, 41*(25), 5236–5248.
Zhang, Z., Zhai, Z. Q., Zhang, W., & Chen, Q. (2007). Evaluation of various turbulence models in predicting airflow and turbulence in enclosed environments by CFD: Part 2 - comparison with experimental data from literature. *HVAC&R Research, 13*, 871–886.
Zhao, X., Shi, Z., & Chen, Q. (2020). Inverse design of an indoor environment using a filter-based topology method with experimental verification. *Indoor Air, 30*, 1039–1051.
Zhao, X., Yin, Y., He, Z., & Liu, X. (2021). Inverse design of indoor radiant terminal using the particle swarm optimization method with topology concept. *Building and Environment, 204*, Article 108117.